


 Cite this: *RSC Adv.*, 2020, **10**, 20778

# *Ab initio* theory study of laser cooling of barium monohalides

 Rong Yang,<sup>a</sup> Bin Tang<sup>b</sup> and XiangYu Han<sup>ac</sup>

The feasibility of laser cooling barium monohalides BaX (X = F, Cl, Br, I) is investigated using *ab initio* methods with the inclusion of spin-orbit coupling (SOC) effects. Calculated spectroscopic constants for BaF, BaCl, BaBr and BaI are in very good agreement with the available experimental measurements. The results demonstrate that the calculated electronic structure is accurate and can be used to establish the optical scheme of laser cooling. The highly diagonal Franck-Condon factors (FCFs) (BaF:  $f_{00} = 0.980$ ,  $f_{11} = 0.939$ ,  $f_{22} = 0.894$ ; BaCl:  $f_{00} = 0.998$ ,  $f_{11} = 0.995$ ,  $f_{22} = 0.992$ ) between the  $X^2\Sigma_{1/2}^+$  and  $A^2\Pi_{1/2}$  states are determined, which are found to be in good agreement with previous theoretical results. The radiative lifetimes (BaF: 39.13–41.20 ns; BaCl: 117.99–110.23 ns) of the  $A^2\Pi_{1/2} - X^2\Sigma_{1/2}^+$  transition for the first five vibrational levels show that the  $A^2\Pi_{1/2}$  is a rather short lifetime state. The current study indicates that BaF and BaCl are two good choices of molecules for laser cooling. Therefore, BaI and BaBr are not promising laser-cooling candidates because the FCFs of the  $A^2\Pi_{1/2} - X^2\Sigma_{1/2}^+$  transition are off-diagonal. We further propose the three-laser cooling schemes based on the  $A^2\Pi_{1/2} - X^2\Sigma_{1/2}^+$  transition for BaF and BaCl.

Received 10th March 2020

Accepted 13th May 2020

DOI: 10.1039/d0ra02211j

[rsc.li/rsc-advances](http://rsc.li/rsc-advances)

## 1. Introduction

The transverse laser cooling of SrF<sup>1,2</sup> and YO<sup>3</sup> has overthrown the notion that laser-cooling molecules is impracticable. The criteria to be considered candidates for laser cooling are a strong transition with highly-diagonal Franck-Condon factors (FCFs) in a wavelength region accessible to tabletop lasers and strong optical forces resulting from the short radiative lifetime. Diagonal FCFs minimize the number of lasers required to keep the molecule in a closed-loop cooling cycle. Naturally, the experimental demonstrations have initiated the search for other molecules which are appropriate for laser cooling. In 2004, Di Rosa<sup>4</sup> conducted a brief survey of promising candidates for laser cooling. SrF and YO did not occur on his study and there clearly could be others that have not been investigated by theoretical and experimental studies. In this paper, thus, we focus on the theoretical studies of the laser cooling of barium monohalides, though neither have yet been cooled.

In recent years, the interest in laser cooling of diatomic polar molecules has grown owing to a variety of prospective applications.<sup>5</sup> Laser cooling of SrF,<sup>1,2</sup> KRb,<sup>6</sup> YO<sup>3</sup> and CaF<sup>7</sup> has been experimentally performed, and polar molecules (such as RaF,<sup>8</sup> AlH,<sup>9</sup> AlF<sup>9</sup>) have been investigated in previous theoretical

research. Alkaline-earth metal atoms and molecules are of persistent interest in the investigation of cold atoms and molecules. These molecules like monohydrides MH (M = Be, Mg, Ca, Sr, and Ba)<sup>10</sup> and some monohalides (such as BeF,<sup>11</sup> MgF<sup>12</sup>) have been identified as the promising candidates for laser cooling theoretically. However, the study on laser cooling of barium monohalides BaX (X = F, Cl, Br, I) is very limited. In addition to being nominated as laser cooling candidates, BaX (X = F, Cl, Br, I) play an important role in stellar spectroscopy.<sup>13</sup> Considering that the  $A^2\Pi \rightarrow X^2\Sigma^+$  transition of barium monohalides has been suggested by Di Rosa<sup>4</sup> and experiments have been made for SrF,<sup>1,2</sup> YO<sup>3</sup> and CaF,<sup>7</sup> we believe it is possible to cool barium monohalides with a similar experimental method.

In the current study, we focus on investigating the feasibility of direct laser cooling of BaX (X = F, Cl, Br, I), then proposing the scheme to perform laser cooling of BaX (X = F, Cl, Br, I). Karthikeyan *et al.*<sup>14</sup> have evaluated the FCFs for electronic transitions A-X of BaF molecule by employing a reliable numerical integration procedure. The calculated FCF ( $f_{00}$ ) of BaF is 0.951, and the laser excitation wavelength is about 857 nm. For BaF, Kang *et al.*<sup>15</sup> also reported results about FCFs by *ab initio*. The radiative lifetime obtained for the  $A^2\Pi$  state of the BaF molecule is  $56.0 \pm 0.9$  ns using laser spectroscopy.<sup>16</sup> The first seven electronic states of the BaCl molecule have been studied by laser induced fluorescence, combined with high resolution Fourier spectroscopy.<sup>17</sup> The zero pressure radiative lifetime of BaCl has been measured by laser-induced fluorescence in the near-infrared wavelength region.<sup>18</sup> Husain *et al.*<sup>19</sup> have determined the spectroscopic parameters of the X-state

<sup>a</sup>School of Mathematics and Physics, Chongqing Jiaotong University, Chongqing 400074, PR China. E-mail: cqjr88@126.com

<sup>b</sup>Institute of Finance & Trade, Chongqing City Management College, Chongqing 401331, PR China

<sup>c</sup>Institute of Atomic and Molecular Physics, Sichuan University, Chengdu 610065, PR China


and low lying excited states of BaBr, and calculated the FCFs using a simplified Morse oscillator model following Tuckett<sup>20</sup> (A-X:  $f_{00} = 0.6903$ ). The  $A^2\Pi$  state of BaBr has been analyzed by Ernst *et al.*<sup>21</sup> Miliordos *et al.*<sup>22</sup> have been examined the electronic structure of BaI by *ab initio* multi-reference configuration interaction (MRCI) and coupled cluster (RCCSD(T)) methods. As mentioned above, BaX (X = F, Cl, Br, I) has been investigated extensively in the past. However, there is a lack of systematic studies of laser cooling of BaX (X = F, Cl, Br, I) up to now.

The paper is organized as follows. The theoretical methods and the basis sets used in the *ab initio* calculations for the included electronic states of BaX (X = F, Cl, Br, I) are briefly described in Section 2. We present the results and data discussions, and propose the laser cooling schemes for BaX (X = F, Cl, Br, I) in Section 3. In Section 4, the conclusions of this work are given.

## 2. Computational details

To investigate the feasibility of direct laser cooling of barium monohalides, we first calculate the electronic structure for the two lowest doublet electronic states ( $A^2\Pi$  and  $X^2\Sigma^+$ ), then determine the radiative properties including radiative lifetimes, FCFs and diode laser excitation wavelengths of the  $A^2\Pi \rightarrow X^2\Sigma^+$  transitions. All the present *ab initio* calculations are carried out in the  $C_{2v}$  point group using the MOLPRO<sup>23</sup> package. The spectroscopic constants, including equilibrium bond distance ( $R_e$ ), harmonic frequency ( $\omega_e$ ), anharmonic vibrational frequency ( $\omega_e\chi_e$ ), rotational constant ( $B_e$ ) and electronic transition energy ( $T_e$ ) for the  $A^2\Pi$  and  $X^2\Sigma^+$  states of BaX (X = F, Cl, Br, I) are evaluated by solving the nuclear Schrödinger equation by Le Roy's LEVEL 8.0 program.<sup>24</sup> With the potential energy curves (PECs) and transition dipole moments of different electronic states, this program can also obtain the FCFs and radiative lifetimes of the various vibrational levels. The FC factor is one of the parameters which controls the intensity distribution in the emission of molecular bands. The square of the overlap integral is termed as FC factor ( $f_{v'v}$ ),<sup>25</sup>

$$f_{v'v} = \left[ \int \psi_{v'} \psi_v dr \right]^2 \quad (1)$$

where  $\psi_{v'}$  and  $\psi_v$  are the vibrational wave functions for the upper and lower states, respectively. The radiative lifetime  $\tau_{v'}$  is calculated by the following formula,

$$\tau_{v'} = \frac{1}{\sum_v A_{v'v}}, \quad (2)$$

where  $A_{v'v}$  is the Einstein A coefficient for the rate of spontaneous emission from initial rovibrational level ( $v', J'$ ) into final rovibrational level ( $v, J$ ),<sup>26,27</sup>

$$A_{v'v} = 3.1361891 \times 10^{-7} \frac{S(J', J)}{2J' + 1} \nu^3 \times \langle \psi_{v'v} | M(r) | \psi_{vJ} \rangle, \quad (3)$$

in the above formula,  $S(J', J)$  is the Hönl–London rotational intensity factor,  $M(r)$  is the transition dipole function,  $\psi_{v'v}$  and  $\psi_{vJ}$  are normalized radial wave functions.

The complete active space self-consistent field (CASSCF)<sup>28,29</sup> and MRCI plus Davidson correction (MRCI + Q)<sup>30–32</sup> methods have been performed for the *ab initio* electronic structure calculations of BaX (X = F, Cl, Br, I). Scalar relativistic effects are accounted for using the Douglas–Kroll–Hess (DHK)<sup>33,34</sup> transformation of the relativistic Hamiltonian. For the heavier Ba atom, the spin–orbit coupling (SOC) effects are important for the electronic structure. In this work, SOC effects are evaluated with one- and two-electrons Breit–Pauli operators<sup>35</sup> at the MRCI level of theory. It is worth noting, we can neglect the rotational degrees of freedom in the first approximation, since we focus on investigating the vibrational cooling.

To improve the accuracy of potential energy curve calculations, the effects of the core–valence correction and the relativistic correlation are taken into account. This was done by adopting the small-core scalar relativistic effective core potential (ECP) ECP10MWB,<sup>36</sup> ECP10MDF,<sup>37</sup> ECP28MDF,<sup>38</sup> and ECP46MDF<sup>39</sup> together with the corresponding valence basis sets for Cl, Br, I and Ba, respectively, and, the AVQZ<sup>40</sup> all-electron basis sets for the F atom. Within the  $C_{2v}$  point group symmetry, all molecular orbitals were labeled by their symmetry ( $a_1, b_1, b_2, a_2$ ). In our calculations of BaF molecule, eight molecular orbitals are selected as active spaces, which correspond to the 2s2p shells of the F atom and 5p6s shells of the Ba atom. That is to say, ten electrons are distributed in a (4, 2, 2, 0) active space for BaF molecule. For BaCl, BaBr and BaI, these active spaces are also (4, 2, 2, 0). The 3s3p shells of the Cl atom, 4s4p shells of the Br atom and 5s5p shells of the Br atom are put in the active space, respectively.

## 3. Results and discussions

### 3.1 Potential energy curves (PECs) and spectroscopic constants

Because the  $A^2\Pi \rightarrow X^2\Sigma^+$  transition has been suggested by experiments for SrF, YO and CaF, we only carry out *ab initio* calculations to the two states ( $A^2\Pi$  and  $X^2\Sigma^+$ ). The PECs of  $A^2\Pi$  and  $X^2\Sigma^+$  states of BaX (X = F, Cl, Br, I) are presented in Fig. 1(a) and (b). Fig. 1 shows that the PECs of  $A^2\Pi$  and  $X^2\Sigma^+$  states look surprisingly similar. It implies that highly diagonal FCFs for the  $A^2\Pi \rightarrow X^2\Sigma^+$  transition are possible.

For the heavier Ba atom, SOC effects are important for the electronic structure. Concerning the effects of SOC on the electronic structure of BaX (X = F, Cl, Br, I), the  $A^2\Pi$  state splits into  $A^2\Pi_{1/2}$  and  $A^2\Pi_{3/2}$ . Our present calculated spectroscopic constants of  $A^2\Pi_{1/2}$  and  $X^2\Sigma^+_{1/2}$  with available experimental values are tabulated in Table 1. The reasons why we focus on  $A^2\Pi_{1/2}$  and  $X^2\Sigma^+_{1/2}$  are explained as follows. Many experimental studies provided some accurate and important spectroscopic data for  $A^2\Pi_{1/2}$  and  $X^2\Sigma^+_{1/2}$  states. Earlier theoretical researches<sup>14,15</sup> reported BaF has highly diagonal FCFs between  $A^2\Pi_{1/2}$  and  $X^2\Sigma^+_{1/2}$ .

For the  $X^2\Sigma^+_{1/2}$  state of BaF, the corresponding percentage errors in  $R_e$ ,  $\omega_e$  and  $\omega_e\chi_e$  are 1.16%, 1.85% and 2.72% with respect to experiment,<sup>41,42</sup> respectively. It is also encouraging to see that our calculated  $T_e$ ,  $R_e$ ,  $\omega_e$  and  $\omega_e\chi_e$  of the  $A^2\Pi_{1/2}$  state are in good agreement with experiment<sup>41,43</sup> and the relative



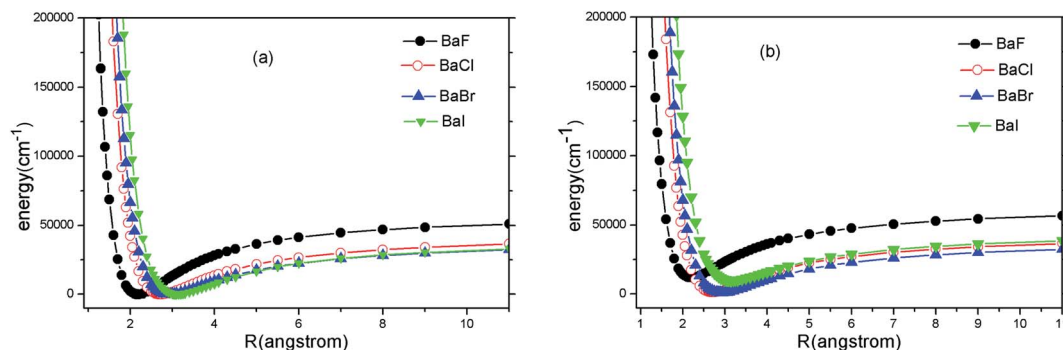


Fig. 1 (Color online) Potential energy curves of X<sup>2</sup>Σ<sup>+</sup><sub>1/2</sub> (a) and A<sup>2</sup>Π<sup>+</sup><sub>1/2</sub> (b) of BaX (X = F, Cl, Br, I) at MRCI + Q/ECP46MDF(Ba), AVQZ(F), ECP10MWB(Cl), ECP10MDF(Br), ECP28MDF(I).

Table 1 Spectroscopic constants of X<sup>2</sup>Σ<sup>+</sup><sub>1/2</sub> and A<sup>2</sup>Π<sup>+</sup><sub>1/2</sub> states of BaX (X = F, Cl, Br, I) calculated at MRCI + Q/ECP46MDF(Ba), AVQZ(F), ECP10MWB(Cl), ECP10MDF(Br), ECP28MDF(I). T<sub>e</sub> is the adiabatic relative electronic energy referred to the ground state, R<sub>e</sub> is the equilibrium internuclear distance, ω<sub>e</sub> and ω<sub>e</sub>χ<sub>e</sub> are the harmonic and anharmonic vibrational frequency, B<sub>e</sub> is the rotational constant

Molecule	States	T <sub>e</sub> (cm <sup>-1</sup> )	R <sub>e</sub> (Å)	ω <sub>e</sub> (cm <sup>-1</sup> )	ω <sub>e</sub> χ <sub>e</sub> (cm <sup>-1</sup> )	B <sub>e</sub> (cm <sup>-1</sup> )	Ref.
BaF	X <sup>2</sup> Σ <sup>+</sup> <sub>1/2</sub>	0	2.186	460.72	1.79	0.2114	This work
		0	2.161 <sup>b</sup>	469.41 <sup>a</sup>	1.84 <sup>a</sup>	—	Expt. ( <sup>a</sup> Ref. 41; <sup>b</sup> Ref. 42)
	A <sup>2</sup> Π <sup>+</sup> <sub>1/2</sub>	11 893	2.199	436.58	1.72	0.2089	This work
		11647 <sup>a</sup>	2.183 <sup>c</sup>	435.50 <sup>a</sup>	1.68 <sup>a</sup>	—	Expt. ( <sup>a</sup> Ref. 41; <sup>c</sup> Ref. 43)
BaCl	X <sup>2</sup> Σ <sup>+</sup> <sub>1/2</sub>	0	2.728	267.38	0.79	0.0814	This work
		0	—	279.89	0.81	0.0840	Expt. (Ref. 17)
	A <sup>2</sup> Π <sup>+</sup> <sub>1/2</sub>	10 657	2.683	261.33	0.80	0.0810	This work
		10 679	—	257.30	0.81	0.0811	Expt. (Ref. 17)
BaBr	X <sup>2</sup> Σ <sup>+</sup> <sub>1/2</sub>	0	2.927	175.14	0.39	0.0390	This work
		0	2.847	192.30	0.41	—	Expt. (Ref. 19)
	A <sup>2</sup> Π <sup>+</sup> <sub>1/2</sub>	10 171	2.911	169.98	0.40	—	This work
		—	2.899	177.13	0.40	—	Expt. (Ref. 19)
BaI	X <sup>2</sup> Σ <sup>+</sup> <sub>1/2</sub>	0	3.126	149.92	0.27	0.0262	This work
		0	3.088	152.16	0.27	—	Expt. (Ref. 44–46)
	A <sup>2</sup> Π <sup>+</sup> <sub>1/2</sub>	9753	3.167	140.47	0.27	0.0255	This work
		9605	3.139	141.75	0.28	—	Expt. (Ref. 45 and 46)

errors are only 2.11%, 0.73%, 0.25% and 2.38%, respectively. In the case of the X<sup>2</sup>Σ<sup>+</sup><sub>1/2</sub> state of BaCl, our present results compare very well with the experimental data<sup>17</sup> (ω<sub>e</sub> ~12.51 cm<sup>-1</sup>, ω<sub>e</sub>χ<sub>e</sub> ~0.02 cm<sup>-1</sup>, B<sub>e</sub> ~0.0026 cm<sup>-1</sup>). And for the A<sup>2</sup>Π<sup>+</sup><sub>1/2</sub> of BaCl, our spectroscopic constants calculated at MRCI level are also in reasonable agreement with experiment<sup>17</sup> (T<sub>e</sub> ~22 cm<sup>-1</sup>, ω<sub>e</sub> ~4.03 cm<sup>-1</sup>, ω<sub>e</sub>χ<sub>e</sub> ~0.01 cm<sup>-1</sup>, B<sub>e</sub> ~0.0001 cm<sup>-1</sup>). Concerning the X<sup>2</sup>Σ<sup>+</sup><sub>1/2</sub> of BaBr, the difference of R<sub>e</sub>, ω<sub>e</sub> and ω<sub>e</sub>χ<sub>e</sub> values in the experiment<sup>19</sup> and present work is not significant, and the relative errors are 2.81%, 8.92% and 4.88%, respectively. While for the A<sup>2</sup>Π<sup>+</sup><sub>1/2</sub> of BaBr, Table 1 shows that our present results accord with experiment<sup>19</sup> (R<sub>e</sub> ~0.012 Å, ω<sub>e</sub> ~7.15 cm<sup>-1</sup>, ω<sub>e</sub>χ<sub>e</sub> ~0.00 cm<sup>-1</sup>). For BaI, present values of R<sub>e</sub>, ω<sub>e</sub> and ω<sub>e</sub>χ<sub>e</sub> for the X<sup>2</sup>Σ<sup>+</sup><sub>1/2</sub> state are 3.126 Å, 140.47 cm<sup>-1</sup> and 0.27 cm<sup>-1</sup>, which are very close to the experimental data.<sup>44–46</sup> Miliordos *et al.*<sup>22</sup> provided a even larger R<sub>e</sub> (3.251 Å) and a even smaller ω<sub>e</sub>χ<sub>e</sub> (0.24 cm<sup>-1</sup>) compared to the experimental data<sup>44–46</sup> by MRCI method. As for the A<sup>2</sup>Π<sup>+</sup><sub>1/2</sub> of BaI, the calculated R<sub>e</sub> and T<sub>e</sub> results are only 0.028 Å and 148 cm<sup>-1</sup> larger, while the ω<sub>e</sub> and ω<sub>e</sub>χ<sub>e</sub> results are only 1.28 cm<sup>-1</sup> and 0.01 cm<sup>-1</sup>

smaller than the observed experimental data.<sup>45,46</sup> The differences between the previous theoretical value<sup>21</sup> and experimental data<sup>45,46</sup> are bigger (T<sub>e</sub> ~1536 cm<sup>-1</sup>, R<sub>e</sub> ~0.194 Å, ω<sub>e</sub> ~12.75 cm<sup>-1</sup>, ω<sub>e</sub>χ<sub>e</sub> ~0.31 cm<sup>-1</sup>). In summary, the results demonstrate that the electronic structure of BaX (X = F, Cl, Br, I) calculated at MRCI + Q/ECP46MDF(Ba), AVQZ(F), ECP10MWB(Cl), ECP10MDF(Br), ECP28MDF(I) level is accurate and can be used to establish the optical scheme of laser cooling.

### 3.2 FCFs

The first criterion to be nominated as candidates for laser cooling is highly diagonal FCFs. As listed in the literature, most FCFs *f*<sub>00</sub> of experimental cooling molecules are greater than 0.9. For example, the FCF *f*<sub>00</sub> of SrF reaches 0.98. A larger FCF has significant benefits for limiting the number of lasers required to keep the molecule in a closed-loop cooling cycle. Of course, some cooling schemes for molecules with smaller FCFs have also been proposed.<sup>47</sup> The FCF values for the A–X transitions of BaX are tabulated in Table 2 and 3. Our computed FCF values of



**Table 2** The calculated FCFs  $f_{\nu\nu}$  of BaF and BaCl for  $A^2\Pi_{1/2}(\nu') \rightarrow X^2\Sigma_{1/2}^+(\nu)$  transitions at MRCI + Q/ECP46MDF(Ba), AVQZ(F), ECP10MWB(Cl) (numbers in bold – published FCF values). Numbers in parentheses indicate the power of 10

Molecules		$\nu' = 0$	1	2	3
BaF	$\nu = 0$	0.9802	0.0197	0.7824(−4)	0.9904(−6)
	Ref. 14 ( <sup>a</sup> Ref. 15)	<b>0.9510, 0.9810<sup>a</sup></b>	<b>0.0490, 0.0189<sup>a</sup></b>	<b>0.0000, 0.3960(−3)<sup>a</sup></b>	0.0000 <sup>a</sup>
	1	0.0194	0.9389	0.0414	0.0030(−1)
	Ref. 14 ( <sup>a</sup> Ref. 15)	<b>0.0480</b>	<b>0.8540, 0.9400<sup>a</sup></b>	<b>0.0960</b>	<b>0.0030</b>
	2	0.0041(−1)	0.0401	0.8937	0.0650
	Ref. 14 ( <sup>a</sup> Ref. 15)	<b>0.0020</b>	<b>0.0930</b>	<b>0.7580, 0.8960<sup>a</sup></b>	<b>0.1410</b>
	3	0.3362(−5)	0.0013	0.0620	0.8452
BaCl	$\nu = 0$	0.9982	0.0017	0.4883(−4)	0.1043(−6)
	1	0.0023	0.9949	0.0032	0.1440(−3)
	2	0.8568(−4)	0.0031	0.9920	0.0045
	3	0.2042(−5)	0.2423(−3)	0.0042	0.9894

**Table 3** The calculated FCFs  $f_{\nu\nu}$  of BaI and BaBr for  $A^2\Pi_{1/2}(\nu') \rightarrow X^2\Sigma_{1/2}^+(\nu)$  transitions at MRCI + Q/ECP46MDF(Ba), ECP10MDF(Br), ECP28MDF(I). Numbers in bold – published FCF values (<sup>a</sup>Ref. 19)

Molecules	$f_{00}f_{01}f_{02}f_{03}$			
	$f_{10}f_{11}f_{12}f_{13}$			
BaI	0.779 0.197 0.023 0.002			
	0.192 0.436 0.307 0.059			
BaBr	0.791( <b>0.690</b> ) <sup>a</sup> 0.189( <b>0.216</b> ) <sup>a</sup> 0.020 0.001			
	0.188( <b>0.260</b> ) <sup>a</sup> 0.440( <b>0.272</b> ) <sup>a</sup> 0.302 0.061			

BaF are in good agreement with the recent results.<sup>14,15</sup> For BaBr, the present results at the MRCI level are a little bigger than the values reported by Husain *et al.*<sup>19</sup> Husain *et al.*<sup>19</sup> calculated the FCFs using a simplified Morse oscillator model following Tuckett. From Table 2, it could be clearly seen that the  $\Delta\nu = 0$  bands of BaX have the strongest transition probability. That is to say, the highly diagonal FCFs  $f_{00}$  (BaF: 0.980 and BaCl: 0.998) for the A–X transition are determined. To visually demonstrate the overlap of the vibrational wave functions for A–X transition, we have plotted the FCFs of spontaneous radiative transitions in Fig. 2. Fig. 2 also shows that BaF and BaCl have large diagonal FCFs.

However for the A–X transition of BaI, the diagonal term  $f_{11}$ (0.436) is calculated, and the off-diagonal term  $f_{10}$ (0.192),  $f_{12}$ (0.307),  $f_{13}$ (0.059) are also obtained (see Table 3). These results show that the A–X transition of BaI does not have highly diagonal FCFs. The calculated  $f_{00}$  of 0.779 for BaI is not large enough to be potentially viable for direct laser cooling. The relative probabilities from  $A^2\Pi_{1/2}(\nu' = 0)$  to  $X^2\Sigma_{1/2}^+(\nu)$  are governed by the FCFs which are about 78% for  $\nu = 0$ , 20% for  $\nu = 1$ , 2.3% for  $\nu = 2$ , 0.2% for  $\nu = 3$ , 0.007% for  $\nu = 4$ , and negligibly small for all  $\nu > 4$ . Five cooling lasers are required for limiting the inefficiency or loss of BaI molecule in the cooling cycle. Cycling transitions requiring one or two repump lasers are common in atomic systems, experimentally. For the A–X transition of BaI, the number of lasers required is not practical. The case of BaBr is similar to the case of BaI (see Table 3). So BaI and

BaBr are not good candidate molecules for direct laser cooling. Thus we do not need to discuss BaI and BaBr molecules in the following section.

### 3.3 Spontaneous radiative lifetime and radiative width

Aside from the large diagonal FCFs, sufficiently short lifetime is desirable for rapid laser cooling. A shorter lifetime of the transition could produce a strong Doppler force, which will produce a significant rate of optical cycling. To produce larger spontaneous scattering forces, the rate of optical cycling ( $10^5$ – $10^8$  s<sup>−1</sup>) is suitable. From eqn (1), the radiative lifetime of vibrational level  $\nu'$  for a given state is given by the inverse of the total Einstein coefficient. The radiative width ( $\Gamma$ ) is related to the lifetime of the state by  $\Gamma = 1/(2\pi c\tau)$ . The computed radiative lifetimes and radiative width of BaF and BaCl are listed in Table 4 for the first five vibrational levels ( $\nu' = 0$ –5). As shown in Table 4, radiative lifetimes increase with increasing  $\nu'$ , and radiative widths decrease with increasing  $\nu'$ . We found that our radiative lifetimes for  $\nu' = 0$  agree well with the experimental results (BaF:  $(56.0 \pm 0.9)$  ns;<sup>16</sup> BaCl:  $(107 \pm 4)$  ns<sup>18</sup>). The radiative lifetimes (BaF: 39.13–41.20 ns; BaCl: 117.99–110.23 ns) of the A–X transition for the first five vibrational levels show that the  $A^2\Pi_{1/2}$  is a rather short lifetime state. Thus, BaF and BaCl meet the second criterion for direct laser cooling.

### 3.4 Laser cooling scheme

As shown in Fig. 3 (a), we have suggested a three-laser cooling scheme for the BaF molecule. The main cycling laser can drive

**Table 4** The calculated radiative lifetimes (ns) and radiative width (cm<sup>−1</sup>) (in bold) for the  $A^2\Pi_{1/2}$  state at MRCI + Q/ECP46MDF(Ba), AVQZ(F), ECP10MWB(Cl)

Molecule	State	$\nu' = 0$	1	2	3	4
BaF	$A^2\Pi_{1/2}$	49.13	49.63	50.15	50.66	51.20
		<b>1.08(−4)</b>	<b>1.07(−4)</b>	<b>1.06(−4)</b>	<b>1.05(−4)</b>	<b>1.04(−4)</b>
BaCl	$A^2\Pi_{1/2}$	117.99	115.95	113.99	112.09	110.23
		<b>4.49(−5)</b>	<b>4.57(−5)</b>	<b>4.64(−5)</b>	<b>4.73(−5)</b>	<b>4.81(−5)</b>



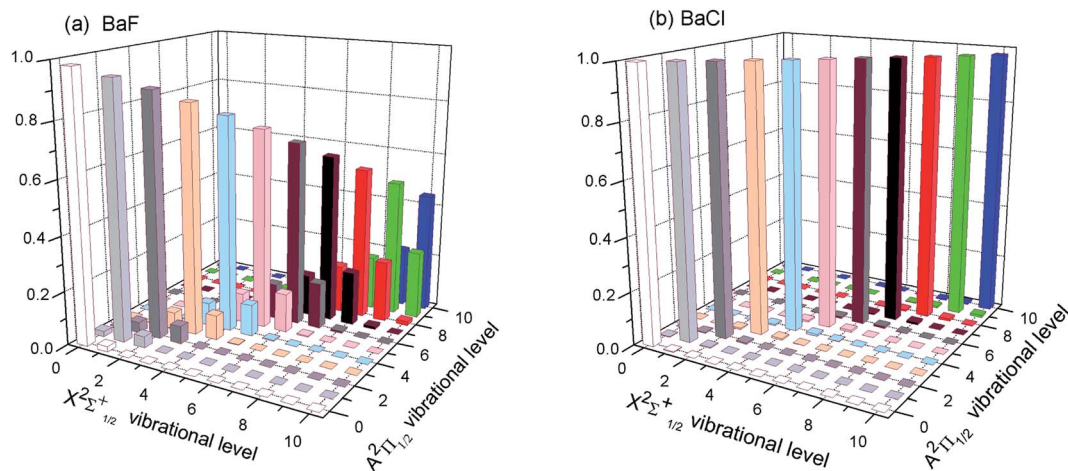


Fig. 2 (Color online) The calculated FCFs of (a) BaF and (b) BaCl for the lowest vibrational levels of the cooling transition  $A^2\Pi_{1/2} \rightarrow X^2\Sigma_{1/2}^+$  at MRCI + Q/ECP46MDF(Ba), AVQZ(F), ECP10MWB(Cl).

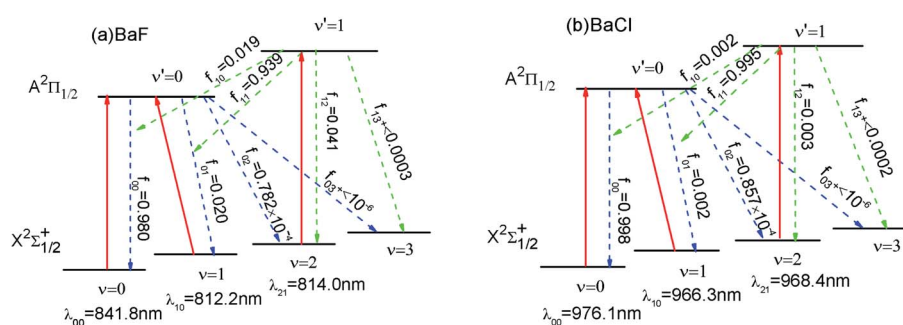


Fig. 3 (Color online) Proposed laser cooling schemes for (a) BaF and (b) BaCl using the  $A^2\Pi_{1/2}(\nu') \rightarrow X^2\Sigma_{1/2}^+(\nu)$  (solid red) transition. The decay pathways with calculated  $f'_{\nu'}$  are shown as dotted line.

the  $X^2\Sigma_{1/2}^+(\nu = 0) \rightarrow A^2\Pi_{1/2}(\nu' = 0)$  transition at wavelength  $\lambda_{00} = 841.8$  nm. Our computed wavelength  $\lambda_{00}$  agrees well with the result (822.0 nm) given by Kang *et al.*<sup>15</sup> However, the decays to the  $X^2\Sigma_{1/2}^+(\nu = 1)$  state, to the  $X^2\Sigma_{1/2}^+(\nu = 2)$  state, and the  $X^2\Sigma_{1/2}^+(\nu \geq 3)$  state from the  $A^2\Pi_{1/2}$  state occur with probability  $f_{01} (= 2\%)$ ,  $f_{02} (\approx 0.008\%)$  and  $f_{03} (< 10^{-6})$ , respectively. To enhance the cooling effect, using the  $X^2\Sigma_{1/2}^+(\nu = 1) \rightarrow A^2\Pi_{1/2}(\nu' = 0)$  transition as the first vibrational pump and the  $X^2\Sigma_{1/2}^+(\nu = 2) \rightarrow A^2\Pi_{1/2}(\nu' = 1)$  transition for the second pump are required. With this scheme, a BaF molecule can scatter about  $N_{\text{scat}} = 1/f_{03} > 10^6$  photons before decaying into the higher vibrational levels ( $\nu \geq 3$ ) in  $X^2\Sigma_{1/2}^+$ . Therefore, two repumping lasers with  $\lambda_{10} = 812.2$  nm and  $\lambda_{21} = 814.0$  nm are needed. The required cooling wavelengths of  $\lambda_{00} = 841.8$  nm,  $\lambda_{10} = 812.2$  nm and  $\lambda_{21} = 814.0$  nm are located in the near-infrared range, where the continuous wavelength laser radiation can be easily generated. One problem with the above laser cooling scheme is the presence of a metastable state  $A^2\Delta$  between the  $X^2\Sigma_{1/2}^+$  and  $A^2\Pi_{1/2}$ .<sup>41</sup> It is notable that the decay rate  $\gamma \propto d^2\omega^3$ . Here the transition dipole moment of A-X ( $d_{AX}$ ) is much larger than that of the A-A' ( $d_{AA'}$ ):  $d_{AX}/d_{AA'} \approx 68$ ,<sup>15</sup> the frequency of A-X ( $\omega_{AX}$ ) is much larger than that of the A-A' ( $\omega_{AA'}$ ):  $\omega_{AX}/\omega_{AA'} \approx 12$ .<sup>41</sup> Thus  $\gamma_{AX}/\gamma_{AA'} \approx 10^6$ . So the presence of the intervening  $A^2\Delta$  state leak is unlikely to limit the laser cooling transition A-X

significantly. The laser cooling of BaCl is similar to that of BaF. In order to avoid or reduce cumbersome problems, here we only show the proposed laser-driven transitions (solid red) and spontaneous decay (dotted line) with calculated  $f'_{\nu'}$  for BaCl in Fig. 3(b).

## 4. Conclusions

In the present work, accurate *ab initio* calculations including the SOC effects are performed on barium monohalides at the MRCI + Q level of theory. The AVQZ basis set (F), pseudopotentials ECPnMDF ( $n = 46, 10, 28$ ) (Ba, Br, I), ECP10MWB(Cl) and corresponding basis sets are used in the present calculations. The PECs for the  $A^2\Pi$  and  $X^2\Sigma^+$  states of BaX (X = F, Cl, Br, I) are presented and analyzed. Our calculated spectroscopic constants ( $R_e, w_e, w_e\chi_e, B_e, T_e$ ) of the  $X^2\Sigma_{1/2}^+$  and  $A^2\Pi_{1/2}$  states are in good agreement with available experimental data. Using the PECs and transition dipole moments, we also obtain the FCFs and radiative lifetimes for the  $X^2\Sigma_{1/2}^+ \rightarrow A^2\Pi_{1/2}$  transition. The results indicate that BaF and BaCl both have highly-diagonal FCFs and short radiative lifetime. Thus BaF and BaCl are promising candidates. The three-laser cooling schemes that drive the  $A^2\Pi_{1/2} \rightarrow X^2\Sigma_{1/2}^+$  transitions have been proposed for BaF and BaCl. However for BaI and BaBr, the A-X transitions do



not have highly diagonal FCFs, and the calculated  $f_{00}$  (BaI: 0.779; BaBr: 0.791) is not large enough to be potentially viable for direct laser cooling. BaI and BaBr are not identified as very promising laser-cooling candidates.

## Conflicts of interest

There are no conflicts to declare.

## Acknowledgements

This work was supported by the National Natural Science Foundation of China (Grant No. 11704052).

## References

- 1 E. S. Shuman, J. F. Barry and D. DeMille, *Nature*, 2010, **467**, 820.
- 2 J. F. Barry, D. J. McCarron, E. B. Norrgard, M. H. Steinecker and D. DeMille, *Nature*, 2014, **512**, 286.
- 3 M. T. Hummon, M. Yeo, B. K. Stuhl, A. L. Collopy, Y. Xia and J. Ye, *Phys. Rev. Lett.*, 2013, **110**, 143001.
- 4 M. D. Di Rosa, *Eur. Phys. J. D*, 2004, **31**, 395.
- 5 L. D. Carr, D. DeMille, R. V. Krems and J. Ye, *New J. Phys.*, 2009, **11**, 055049.
- 6 J. Kobayashi, K. Aikawa, K. Oasa and S. Inouye, *Phys. Rev. A*, 2014, **89**, 021401(R).
- 7 V. Zhelyazkova, A. Cournol, T. E. Wall, A. Matsushima, J. J. Hudson, E. A. Hinds, M. R. Tarbutt and B. E. Sauer, *Phys. Rev. A*, 2014, **89**, 053416.
- 8 T. A. Isaev, S. Hoekstra and R. Berger, *Phys. Rev. A*, 2010, **82**, 052521.
- 9 N. Wells and I. C. Lane, *Phys. Chem. Chem. Phys.*, 2011, **13**, 19018.
- 10 Y. F. Gao and T. Gao, *Phys. Rev. A*, 2014, **90**, 052506.
- 11 I. C. Lane, *Phys. Chem. Chem. Phys.*, 2012, **14**, 15078.
- 12 S. Y. Kang, Y. F. Gao, F. G. Kuang, T. Gao, J. G. Du and G. Jiang, *Phys. Rev. A*, 2015, **91**, 042511.
- 13 H. Holweger and E. A. Mueller, *Sol. Phys.*, 1974, **39**, 19.
- 14 B. Karthikeyan, K. Balachandrakumar, V. Raja and N. Rajamanickam, *J. Appl. Spectrosc.*, 2013, **80**, 5.
- 15 S. Y. Kang, F. G. Kuang, G. Jiang and J. G. Du, *Mol. Phys.*, 2016, **114**, 810.
- 16 L. E. Berg, N. Gador, D. Husain, H. Ludwigs and P. Royen, *Chem. Phys. Lett.*, 1998, **287**, 89.
- 17 C. Amiot, M. Hafid and J. Vergès, *J. Mol. Spectrosc.*, 1996, **180**, 121.
- 18 A. Derkatch, C. Lundevall, L.-E. Berg and P. Royen, *Chem. Phys. Lett.*, 2000, **332**, 278.
- 19 D. Husain, J. Lei, F. Castano and M. N. Sánchez Rayo, *J. Photochem. Photobiol. Chem.*, 1997, **107**, 1.
- 20 R. P. Tuckett, personal communication, 1992.
- 21 W. E. Ernst, G. Weller and T. Topping, *Chem. Phys. Lett.*, 1985, **121**, 6.
- 22 E. Miliordos, A. Papakondylis, A. A. Tsekouras and A. Mavridis, *J. Phys. Chem. A*, 2007, **111**, 10002.
- 23 H.-J. Werner, P. J. Knowles, R. Lindh, F. R. Manby and M. Schütz, *et al.*, *MOLPRO, is a package of ab initio programs, version 2009.1*, <http://www.molpro.net>.
- 24 R. J. Le Roy, LEVEL 8.0, A Computer Program for Solving the Radial Schrödinger Equation for Bound and Quasibound Levels, *CPRR-663*, University of Waterloo, Waterloo, ON, 2007.
- 25 D. R. Bates, *Mon. Not. Roy. Astron. Soc.*, 1952, **112**, 614.
- 26 G. Herzberg, *Spectra of Diatomic Molecules*, Van Nostrand, New York, 1950.
- 27 P. F. Bernath, *Spectra of Atoms and Molecules*, Oxford University Press, New York, 2nd ed, 2005.
- 28 H.-J. Werner and P. J. Knowles, *J. Chem. Phys.*, 1985, **82**, 5053.
- 29 P. J. Knowles and H.-J. Werner, *Chem. Phys. Lett.*, 1985, **115**, 259.
- 30 H.-J. Werner and P. J. Knowles, *J. Chem. Phys.*, 1988, **89**, 5803.
- 31 P. J. Knowles and H.-J. Werner, *Chem. Phys. Lett.*, 1988, **145**, 514.
- 32 S. R. Langhoff and E. R. Davidson, *Int. J. Quantum Chem.*, 1974, **8**, 61.
- 33 N. Douglas and N. M. Kroll, *Ann. Phys.*, 1974, **82**, 89.
- 34 B. A. Hess, *Phys. Rev. A*, 1986, **33**, 3742.
- 35 A. Berning, M. Schweizer, H.-J. Werner, P. J. Knowles and P. Palmieri, *Mol. Phys.*, 2000, **98**, 1823.
- 36 A. Bergner, M. Dolg, W. Kuechle, H. Stoll and H. Preuss, *Mol. Phys.*, 1993, **80**, 1431.
- 37 K. A. Peterson, D. Figgen, E. Goll, H. Stoll and M. Dolg, *J. Chem. Phys.*, 2003, **119**, 11113.
- 38 K. A. Peterson, B. C. Shepler, D. Figgen and H. Stoll, *J. Phys. Chem. A*, 2006, **110**, 13877.
- 39 I. S. Lim, H. Stoll and P. Schwerdtfeger, *J. Chem. Phys.*, 2006, **124**, 034107.
- 40 A. K. Wilson, D. E. Woon, K. A. Peterson and T. H. Dunning Jr, *J. Chem. Phys.*, 1999, **110**, 7667.
- 41 R. F. Barrow, A. Bernard, C. Effantin, J. D'incan, G. Fabre, A. E. Hachimi, R. Stringat and J. Vergès, *Chem. Phys. Lett.*, 1988, **147**, 535.
- 42 C. Ryzlewicz and T. Topping, *Chem. Phys.*, 1980, **51**, 329.
- 43 K. P. Huber and G. Herzberg, *Molecular Spectra and Molecular Structure IV: Constants of Diatomic Molecules*, Van Nostrand-Reinhold, 2005.
- 44 R. F. Gutterres, J. Vergès and C. Amiot, *J. Mol. Spectrosc.*, 1999, **196**, 29.
- 45 R. F. Gutterres, J. Vergès and C. Amiot, *J. Mol. Spectrosc.*, 2000, **200**, 253.
- 46 R. F. Gutterres, J. Vergès and C. Amiot, *J. Mol. Spectrosc.*, 2001, **206**, 62.
- 47 R. Yang, Y. F. Gao, B. Tang and T. Gao, *Phys. Chem. Chem. Phys.*, 2015, **17**, 1900.

